

7.7 Kirchhoff Theory[†]

A more rigorous treatment of Huygens' principle was given by Kirchhoff and forms the basis for a number of important techniques for computing synthetic seismograms. Descriptions of applications of Kirchhoff methods to seismology may be found in Scott and Helmberger (1983) and Kampmann and Müller (1989). Kirchhoff theory was first developed in optics and our derivation until Equation (7.56) largely follows that of Longhurst (1967). Consider the scalar wave equation (e.g., Equation (3.31) where ϕ is the P -wave potential)

$$\nabla^2 \phi = \frac{1}{c^2} \frac{\partial^2 \phi}{\partial t^2}, \quad (7.35)$$

where c is the wave velocity. Now assume a harmonic form for ϕ , that is, at a particular frequency ω we have the monochromatic function

$$\phi = \psi(\mathbf{r})e^{-i\omega t} = \psi(\mathbf{r})e^{-ikct}, \quad (7.36)$$

where \mathbf{r} is the position and $k = \omega/c$ is the wavenumber. Note that we have separated the spatial and temporal parts of ϕ . We then have

$$\nabla^2 \phi = e^{-ikct} \nabla^2 \psi \quad (7.37)$$

and

$$\frac{\partial^2 \phi}{\partial t^2} = -k^2 c^2 \psi e^{-ikct} \quad (7.38)$$

and (7.35) becomes

$$\nabla^2 \psi = -k^2 \psi. \quad (7.39)$$

This is a time-independent wave equation for the space-dependent part of ϕ . It is also sometimes termed the Helmholtz equation.

Next, recall Green's theorem from vector calculus. If ψ_1 and ψ_2 are two continuous single-valued functions with continuous derivatives, then for a closed surface S

$$\int_V (\psi_2 \nabla^2 \psi_1 - \psi_1 \nabla^2 \psi_2) dv = \int_S \left(\psi_2 \frac{\partial \psi_1}{\partial n} - \psi_1 \frac{\partial \psi_2}{\partial n} \right) dS, \quad (7.40)$$

where the volume integral is over the volume enclosed by S , and $\partial/\partial n$ is the derivative with respect to the outward normal vector to the surface. Now assume that both ψ_1 and ψ_2 satisfy (7.39), that is,

$$\nabla^2 \psi_1 = -k^2 \psi_1, \quad (7.41)$$

$$\nabla^2 \psi_2 = -k^2 \psi_2. \quad (7.42)$$

In this case, the left part of (7.40) vanishes and the surface integral must be zero:

$$\int_S \left(\psi_2 \frac{\partial \psi_1}{\partial n} - \psi_1 \frac{\partial \psi_2}{\partial n} \right) dS = 0. \quad (7.43)$$

Now suppose that we are interested in evaluating the disturbance at the point P , which is enclosed by the surface S (Fig. 7.16). We set $\psi_1 = \psi$, the amplitude of the harmonic disturbance. We are free to choose any function for ψ_2 , provided it also satisfies (7.39). It will prove useful to define ψ_2 as

$$\psi_2 = \frac{e^{ikr}}{r}, \quad (7.44)$$

where r is the distance from P . This function has a singularity at $r = 0$ and so the point P must be excluded from the volume integral for Green's theorem to be valid. We can do this by placing a small sphere Σ around P . Green's theorem may

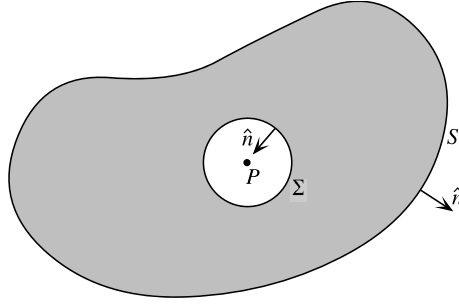


Figure 7.16: A point P surrounded by a surface S of arbitrary shape. Kirchhoff's formula is derived by applying Green's theorem to the volume between S and an infinitesimal sphere Σ surrounding P .

now be applied to the volume between Σ and S ; these surfaces, together, make up the integration surface. On the surface of the small sphere the outward normal to this volume is opposite to the direction of r and thus $\partial/\partial n$ can be replaced with $-\partial/\partial r$ and the surface integral over Σ may be expressed as

$$\begin{aligned} \int_{\Sigma} \left(\psi_2 \frac{\partial \psi}{\partial n} - \psi \frac{\partial \psi_2}{\partial n} \right) dS &= \int_{\Sigma} \left[\frac{-e^{ikr}}{r} \frac{\partial \psi}{\partial r} + \psi \frac{\partial}{\partial r} \left(\frac{e^{ikr}}{r} \right) \right] dS \\ &= \int_{\Sigma} \left[\frac{-e^{ikr}}{r} \frac{\partial \psi}{\partial r} + \psi \left(\frac{-e^{ikr}}{r^2} + \frac{ike^{ikr}}{r} \right) \right] dS. \end{aligned} \quad (7.45)$$

Now let us change this to an integral over solid angle Ω from the point P , in which dS on Σ subtends $d\Omega$ and $dS = r^2 d\Omega$. Then

$$\int_{\Sigma} = \int_{\text{around } P} \left(-re^{ikr} \frac{\partial \psi}{\partial r} - \psi e^{ikr} + rik\psi e^{ikr} \right) d\Omega. \quad (7.46)$$

Now consider the limit as r goes to zero. Assuming that ψ does not vanish, then only the second term in this expression survives. Thus as $r \rightarrow 0$

$$\int_{\Sigma} \rightarrow \int -\psi e^{ikr} d\Omega. \quad (7.47)$$

As the surface Σ collapses around P , the value of ψ on the surface may be assumed to be constant and equal to ψ_P , its value at P . Thus

$$\int_{\Sigma} \rightarrow \int -\psi_P e^{ikr} d\Omega \quad (7.48)$$

$$= -\psi_P \int e^{ikr} d\Omega \quad (7.49)$$

$$= -\psi_P \int d\Omega \quad \text{since } e^{ikr} \rightarrow 1 \text{ as } r \rightarrow 0 \quad (7.50)$$

$$= -4\pi\psi_P. \quad (7.51)$$

From (7.43) we know that $\int_{S+\Sigma} = 0$, so we must have $\int_S = +4\pi\psi_P$, or

$$4\pi\psi_P = \int_S \left[\frac{e^{ikr}}{r} \frac{\partial \psi}{\partial n} - \psi \frac{\partial}{\partial n} \left(\frac{e^{ikr}}{r} \right) \right] dS \quad (7.52)$$

$$= \int_S \left[\frac{e^{ikr}}{r} \frac{\partial \psi}{\partial n} - \psi e^{ikr} \frac{\partial}{\partial n} \left(\frac{1}{r} \right) - \frac{ik\psi e^{ikr}}{r} \frac{\partial r}{\partial n} \right] dS, \quad (7.53)$$

since $\frac{\partial}{\partial n} = \frac{\partial}{\partial r} \frac{\partial r}{\partial n}$. This is often called Helmholtz's equation. Since $\phi = \psi e^{-ikct}$ (Equation 7.35), we have

$$\psi = \phi e^{ikct} \quad (7.54)$$

and (7.53) becomes

$$\begin{aligned} \phi_P &= \frac{1}{4\pi} e^{-ikct} \int_S \left[\frac{e^{ikr}}{r} \frac{\partial \psi}{\partial n} - \psi e^{ikr} \frac{\partial}{\partial n} \left(\frac{1}{r} \right) - \frac{ik\psi e^{ikr}}{r} \frac{\partial r}{\partial n} \right] dS \\ &= \frac{1}{4\pi} \int_S \left[\frac{e^{-ik(ct-r)}}{r} \frac{\partial \psi}{\partial n} - \psi e^{-ik(ct-r)} \frac{\partial}{\partial n} \left(\frac{1}{r} \right) - \frac{ik\psi e^{-ik(ct-r)}}{r} \frac{\partial r}{\partial n} \right] dS. \end{aligned} \quad (7.55)$$

This expression gives $\phi(t)$ at the point P . Note that the term $\psi e^{-ik(ct-r)} = \psi e^{-ikc(t-r/c)}$ is the value of ϕ at the element dS at the time $t - r/c$. This time is referred to as the *retarded value* of ϕ and is written $[\phi]_{t-r/c}$. In this way, we can express (7.55) as

$$\phi_P = \frac{1}{4\pi} \int_S \left(\frac{1}{r} \left[\frac{\partial \phi}{\partial n} \right]_{t-r/c} - \frac{\partial}{\partial n} \left(\frac{1}{r} \right) [\phi]_{t-r/c} + \frac{1}{cr} \frac{\partial r}{\partial n} \left[\frac{\partial \phi}{\partial t} \right]_{t-r/c} \right) dS, \quad (7.56)$$

where we have used $\partial \phi / \partial t = -ikc\psi e^{-ikct}$. Equation (7.56) is a standard form for what is often termed Kirchhoff's formula; it is found in many optics textbooks and is also given in Scott and Helmberger (1983). We see that the disturbance at P can be computed from the conditions of ϕ over a closed surface surrounding P where r/c represents the time taken for the disturbance to travel the distance r from dS to P .

We need to know both the value of ϕ and its normal derivative on dS to compute this integral.

This is not an especially convenient form to use directly in most seismic applications. Suppose the value of ϕ at each point on the surface could be obtained from a source time function $f(t)$ a distance r_0 from dS . Then on dS we have

$$\phi = \frac{1}{r_0} f(t - r_0/c), \quad (7.57)$$

$$\frac{\partial \phi}{\partial t} = \frac{1}{r_0} f'(t - r_0/c), \quad (7.58)$$

where the $1/r_0$ term comes from the geometrical spreading of the wavefront.

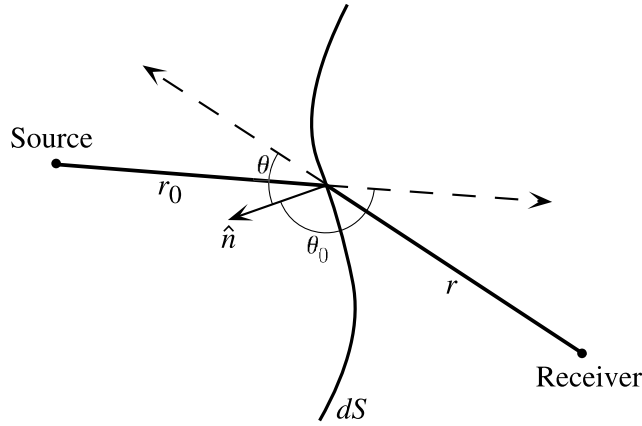


Figure 7.17: The ray geometry for a single point on a surface dS separating a source and receiver.

If θ_0 and θ are the angles of the incoming and outgoing ray paths from the surface normal (Fig. 7.17), then

$$\frac{\partial r_0}{\partial n} = \cos \theta_0 \quad \text{and} \quad \frac{\partial r}{\partial n} = \cos \theta, \quad (7.59)$$

$$\frac{\partial \phi}{\partial n} = \frac{\partial \phi}{\partial r_0} \frac{\partial r_0}{\partial n} \quad (7.60)$$

$$= \frac{\partial \phi}{\partial r_0} \cos \theta_0, \quad (7.61)$$

and

$$\frac{\partial}{\partial n} \left(\frac{1}{r} \right) = \frac{\partial r}{\partial n} \frac{\partial}{\partial r} \left(\frac{1}{r} \right) \quad (7.62)$$

$$= -\frac{1}{r^2} \cos \theta. \quad (7.63)$$

We can evaluate $\partial \phi / \partial r_0$ using the chain rule:

$$\frac{\partial}{\partial r_0} \left(\frac{1}{r_0} f(t - r_0/c) \right) = -\frac{1}{r_0^2} f(t - r_0/c) - \frac{1}{cr_0} f'(t - r_0/c) \quad (7.64)$$

since $\frac{\partial}{\partial r_0} = \frac{\partial t}{\partial r_0} \frac{\partial}{\partial t} = -\frac{1}{c} \frac{\partial}{\partial t}$. Putting (7.57)–(7.64) into (7.56), we have

$$\begin{aligned}\phi_P(t) &= \frac{1}{4\pi} \int_S \left(\frac{-1}{rr_0^2} \cos \theta_0 + \frac{1}{r^2 r_0} \cos \theta \right) f(t - r/c - r_0/c) dS \\ &\quad + \frac{1}{4\pi} \int_S \left(\frac{-1}{crr_0} \cos \theta_0 + \frac{1}{crr_0} \cos \theta \right) f'(t - r/c - r_0/c) dS.\end{aligned}\quad (7.65)$$

The negative signs arise from our definition of \hat{n} in the direction opposing r_0 ; these terms are positive since $\cos \theta_0$ is negative. Equation (7.65) may also be expressed in terms of convolutions with $f(t)$ and $f'(t)$:

$$\begin{aligned}\phi_P(t) &= \frac{1}{4\pi} \int_S \delta \left(t - \frac{r + r_0}{c} \right) \left(\frac{-1}{rr_0^2} \cos \theta_0 + \frac{1}{r^2 r_0} \cos \theta \right) dS * f(t) \\ &\quad + \frac{1}{4\pi} \int_S \delta \left(t - \frac{r + r_0}{c} \right) \left(\frac{-1}{crr_0} \cos \theta_0 + \frac{1}{crr_0} \cos \theta \right) dS * f'(t).\end{aligned}\quad (7.66)$$

Notice that the $f(t)$ terms contain an extra factor of $1/r$ or $1/r_0$. For this reason they are most important close to the surface of integration and can be thought of as near-field terms. In practice, the source and receiver are usually sufficiently distant from the surface (i.e., $\lambda \ll r, r_0$) that ϕ_P is well approximated by using only the far-field $f'(t)$ terms. In this case we have

$$\phi_P(t) = \frac{1}{4\pi c} \int_S \delta \left(t - \frac{r + r_0}{c} \right) \frac{1}{rr_0} (-\cos \theta_0 + \cos \theta) dS * f'(t).\quad (7.67)$$

This formula is the basis for many computer programs that compute Kirchhoff synthetic seismograms.

7.7.1 Kirchhoff applications

Probably the most common seismic application of Kirchhoff theory involves the case of an irregular interface between simpler structure on either side. Kirchhoff theory can be used to provide an approximate solution for either the transmitted or reflected wavefield due to this interface (Fig. 7.18).

For example, we might want to model the effect of irregularities on the core–mantle boundary, the Moho, the sea floor, or a sediment–bedrock interface. In each case, there is a significant velocity contrast across the boundary.

Let us consider the reflected wave generated by a source above an undulating interface. Assume that the incident wavefield is known and can be described with geometrical ray theory. Then we make the approximation that the reflected wavefield just above the interface is given by the plane-wave reflection coefficient for the ray incident on the surface. This approximation is sometimes called the Kirchhoff, physical optics, or tangent plane hypothesis (Scott and Helmberger, 1983). Each point on the surface reflects the incident pulse as if there were an infinite plane

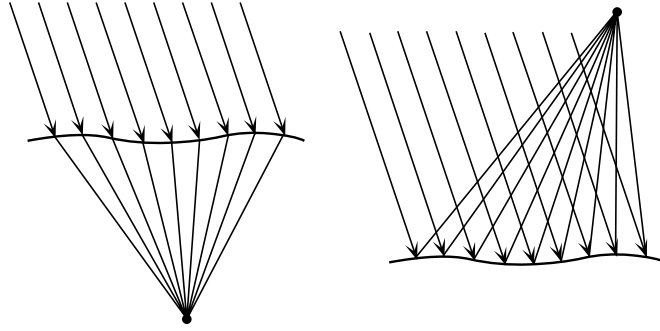


Figure 7.18: Kirchhoff theory can be used to compute the effect of an irregular boundary on both transmitted and reflected waves.

tangent to the surface at that point. Considering only the far-field terms, we then have

$$\phi_P(t) = \frac{1}{4\pi c} \int_S \delta \left(t - \frac{r + r_0}{c} \right) \frac{R(\theta_0)}{rr_0} (\cos \theta_0 + \cos \theta) dS * f'(t), \quad (7.68)$$

where $R(\theta_0)$ is the reflection coefficient, θ_0 is the angle between the incident ray and the surface normal, and θ is the angle between the scattered ray and the surface normal (see Fig. 7.19).

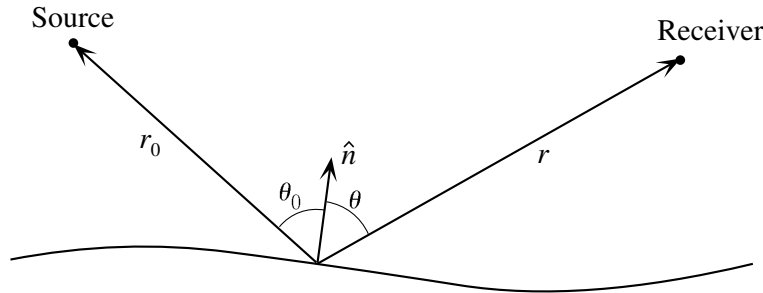


Figure 7.19: Ray angles relative to the surface normal for a reflected wave geometry.

If the overlying layer is not homogeneous, then the $1/r$ and $1/r_0$ terms must be replaced with the appropriate source-to-interface and interface-to-receiver geometrical spreading coefficients. In some cases, particularly for obliquely arriving rays, the reflection coefficient R may become complex. If this occurs, then this equation will have both a real and an imaginary part. The final time series is obtained by adding the real part to the Hilbert transform of the imaginary part.

The Kirchhoff solution will correctly model much of the frequency dependence and diffracted arrivals in the reflected wavefield. These effects are not obtained through geometrical ray theory alone, even if 3-D ray tracing is used. For example, consider a source and receiver above a horizontal interface containing a vertical fault (Fig. 7.20).

Geometrical ray theory will produce only the main reflected pulse from the interface, while Kirchhoff theory will provide both the main pulse and the secondary pulse diffracted from the corner. However, Kirchhoff theory also has its limitations,

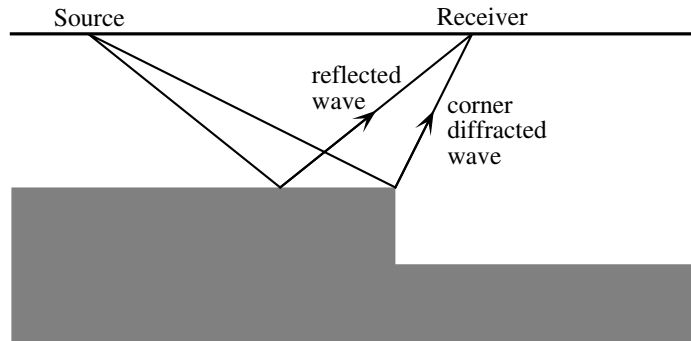


Figure 7.20: This structure will produce both a direct reflected pulse and a diffracted pulse for the source–receiver geometry shown.

in that it does not include any multiple scattering or diffractions along the interface; these might be important in more complicated examples.

7.7.2 How to write a Kirchhoff program

As an illustration, let us list the steps involved in writing a hypothetical Kirchhoff computer program to compute the reflected wavefield from a horizontal interface with some irregularities.

1. Specify the source and receiver locations.
2. Specify the source-time function $f(t)$.
3. Compute $f'(t)$, the derivative of the source-time function.
4. Initialize to zero a time series $J(t)$, with sample interval dt , that will contain the output of the Kirchhoff integral.
5. Specify the interface with a grid of evenly spaced points in x and y . At each grid point, we must know the height of the boundary z and the normal vector to the surface \hat{n} . We also require the surface area, dA , corresponding to the grid point. This is approximately $dx dy$ where dx and dy are the grid spacings in the x and y directions, respectively (if a significant slope is present at the grid point, the actual surface area is greater and this correction must be taken into account). The grid spacing should be finer than the scale length of the irregularities.
6. At each grid point, trace rays to the source and receiver. Determine the travel times to the source and receiver, the ray angles to the local normal vector (θ_0 and θ), and the geometrical spreading factors g_0 (source-to-surface) and g (surface-to-receiver).
7. At each grid point, compute the reflection coefficient $R(\theta_0)$ and the factor $\cos \theta_0 + \cos \theta$.

8. At each grid point, compute the product $R(\theta_0)(\cos \theta_0 + \cos \theta)dA/(4\pi cg_0g)$. Add the result to the digitized point of $J(t)$ that is closest to the total source-surface-receiver travel time, after first dividing the product by the digitization interval dt .
9. Repeat this for all grid points that produce travel times within the time interval of interest.
10. Convolve $J(t)$ with $f'(t)$, the derivative of the source-time function, to produce the final synthetic seismogram.
11. (very important) Repeat this procedure at a finer grid spacing, dx and dy , to verify that the same result is obtained. If not, the interface is undersampled and a finer grid must be used.

Generally the $J(t)$ function will contain high-frequency numerical “noise” that is removed through the convolution with $f'(t)$. It is computationally more efficient to compute $f'(t)$ and convolve with $J(t)$ than to compute $J'(t)$ and convolve with $f(t)$, particularly when multiple receiver positions are to be modeled.

7.7.3 Kirchhoff migration

Kirchhoff results can be used to implement migration methods for reflection seismic data that are consistent with wave propagation theory. For zero-offset data, $\theta_0 = \theta$ and $r_0 = r$ and Equation (7.68) becomes

$$\phi_P(t) = \frac{1}{2\pi c} \int_S \delta\left(t - \frac{r + r_0}{c}\right) \frac{R(\theta_0)}{r^2} \cos \theta dS * f'(t). \quad (7.69)$$

To perform the migration, the time derivative of the data is taken and the traces for each hypothetical scattering point are multiplied by the obliquity factor $\cos \theta$, scaled by the spherical spreading factor $1/r^2$ and then summed along the diffraction hyperbolas.

7.8 EXERCISES

1. (COMPUTER) Recall Equation (7.17) for the vibroseis sweep function:

$$v(t) = A(t) \sin[2\pi(f_0 + bt)t].$$

- (a) Solve for f_0 and b in the case of a 20-s long sweep between 1 and 4 Hz. Hint: $b = 20/3$ is incorrect! Think about how rapidly the phase changes with time.
- (b) Compute and plot $v(t)$ for this sweep function. Assume that $A(t) = \sin^2(\pi t/20)$ (this is termed a Hanning taper; note that it goes smoothly to zero at $t = 0$ and $t = 20$ s). Check your results and make sure that you have the right period at each end of the sweep.

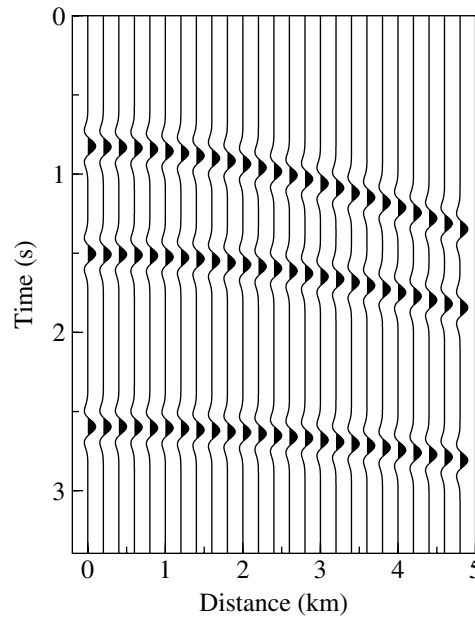


Figure 7.21: P -wave reflections from an individual CMP gather. Note the increase of travel time with source–receiver distance.

- (c) Compute and plot the autocorrelation of $v(t)$ between -2 and 2 s.
 - (d) Repeat (b) and (c), but this time assume that $A(t)$ is only a short 2-s long taper at each end of the sweep, that is, $A(t) = \sin^2(\pi t/4)$ for $0 < t < 2$, $A(t) = 1$ for $2 \leq t \leq 18$, and $A(t) = \sin^2[\pi(20 - t)/4]$ for $18 < t < 20$. Note that this milder taper leads to more extended sidelobes in the autocorrelation function.
 - (e) What happens to the pulse if autocorrelation is applied a second time to the autocorrelation of $v(t)$? To answer this, compute and plot $[v(t) \star v(t)] \star [v(t) \star v(t)]$ using $v(t)$ from part (b). Is this a way to produce a more impulsive wavelet?
2. A reflection seismic experiment produces the CMP gather plotted in Figure 7.21. Using the $t^2(x^2)$ method, determine the approximate rms velocity of the material overlying each reflector. Then compute an approximate depth to each reflector. Note: You should get approximately the same velocity for each reflector; do not attempt to solve for different velocities in the different layers.
 3. Consider a simple homogeneous layer over half-space model (as plotted in Fig. 7.22) with P velocity α_1 and S velocity β_1 in the top layer and P velocity α_2 in the bottom layer.
 - (a) Assuming a layer thickness of h and a ray parameter of p , derive an equation for the differential time ($T_{Ps} - T_P$) between P and Ps at the

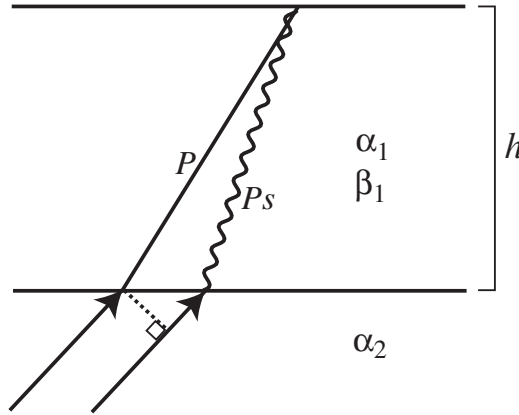


Figure 7.22: The P and P_s ray geometry for an upcoming plane wave incident on a constant velocity layer.

surface. Hint: the travel time is equal along the wavefront shown by the dashed line in the bottom layer.

- (b) What is $T_{P_s} - T_P$ for $h = 40$ km, $\alpha_1 = 6.3$ km/s, $\beta_1 = 3.6$ km/s, $\alpha_2 = 8$ km/s, and $p = 0.06$ s/km?
4. (COMPUTER) A common pulse shape used in reflection seismic modeling is the *Ricker wavelet*, defined as

$$s_R(t) = \left(1 - 2\pi^2 f_p^2 t^2\right) e^{-\pi^2 f_p^2 t^2}, \quad (7.70)$$

where f_p is the peak frequency in the spectrum of the wavelet.

- (a) Using a digitization rate of 200 samples/s and assuming $f_p = 4$ Hz, make a plot of $s_R(t)$ and its time derivative between -0.5 and 0.5 s.
- (b) Following Huygens' principle, model the plane reflector shown in Figure 7.23 as a large number of point sources. Use a velocity of 4 km/s, and a coincident source and receiver located 2 km from the center of a 10 km by 10 km plane, with secondary Huygens sources spaced every 0.1 km on the plane (i.e., 101 points in each direction, for a total of 10,201 sources). Construct and plot a synthetic seismogram representing the receiver response to the Ricker wavelet from part (a) by summing the contribution from each secondary source. At each point, compute the two-way travel time from/to the source/receiver and the geometric spreading factor $1/r^2$. Add the Ricker wavelet, centered on the two-way time and scaled by the geometric spreading factor, to your synthetic time series for each of the 10,201 points. Note that the resulting waveform for the reflected pulse is *not* the same shape as the Ricker wavelet.
- (c) Repeat part (b), but this time use the Kirchhoff result that the secondary sources are given by the derivative of the Ricker wavelet. Assume that $R(\theta) = 1$ for this example. Show that the synthetic reflected pulse has the correct shape.

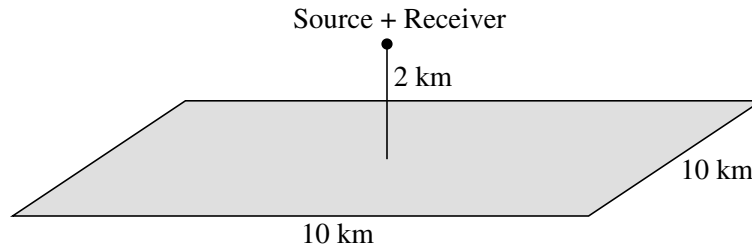


Figure 7.23: The geometry for Problem 7.4, constructing a reflected pulse as a sum of secondary sources.

- (d) Verify that the reflected pulse from part (c) has an amplitude of 0.25, the same as the predicted amplitude of a pulse 4 km away from a point source that has unit amplitude at $r = 1$.
- (e) Note: Because convolution is a linear operation, parts (b) and (c) can be performed more efficiently by summing over the 10,201 points assuming a simple spike source ($s(t) = 1/r^2$ at the $t = 0$ point only) and then convolving the resulting time series with the Ricker wavelet or its time derivative to obtain the final synthetic seismogram. The intermediate time series will contain considerable high frequency noise but this is removed by the convolution.
- (f) The main reflected pulse should arrive at $t = 1$ s. What is the origin of the small pulse at about 2.7 s?